

Structural and electrical properties of $(\text{Ti}_{0.9}\text{Zr}_{0.1})\text{Si}_2$ thin films on Si(111)

Cite as: Appl. Phys. Lett. **65**, 2413 (1994); <https://doi.org/10.1063/1.112692>

Submitted: 07 June 1994 • Accepted: 12 September 1994 • Published Online: 04 June 1998

Y. Dao, A. M. Edwards, H. Ying, et al.



[View Online](#)



[Export Citation](#)

 QBLOX



1 qubit

Shorten Setup Time
Auto-Calibration
More Qubits

Fully-integrated
Quantum Control Stacks
Ultrastable DC to 18.5 GHz
Synchronized <<1 ns
Ultralow noise



100s qubits

[visit our website >](#)

AIP
Publishing

Structural and electrical properties of $(\text{Ti}_{0.9}\text{Zr}_{0.1})\text{Si}_2$ thin films on Si(111)

Y. Dao, A. M. Edwards, H. Ying, Y. L. Chen, D. E. Sayers, and R. J. Nemanich
Department of Physics, North Carolina State University, Raleigh, North Carolina 27695-8202

(Received 7 June 1994; accepted for publication 12 September 1994)

Alloy films of Ti and up to 20% Zr were prepared by codeposition onto Si(111) surfaces in ultrahigh vacuum. After *in situ* thermal annealing at temperatures of $\sim 600^\circ\text{C}$, the films form the C49 phase and are stable in this phase up to at least 910°C . In contrast, Ti films on Si(111) initially react to form the C49 phase and transform to the C54 phase at $\sim 700^\circ\text{C}$. The surfaces of the $(\text{Ti}_{0.9}\text{Zr}_{0.1})\text{Si}_2$ alloy films are studied by atomic force microscopy and are shown to be smoother than the surfaces of TiSi_2 films on Si substrates. In addition the tendency to island formation is also not observed for annealing temperatures less than 910°C . The sheet resistivity of the $(\text{Ti}_{0.9}\text{Zr}_{0.1})\text{Si}_2$ alloy films is found to be $\sim 46\ \mu\Omega\text{ cm}$ for annealing temperatures from 600 to 910°C . © 1994 American Institute of Physics.

Refractory metal silicides are often considered for contacts and interconnections in very large scale integrated circuits. Compared to other metal silicides, TiSi_2 has a relatively low electrical resistivity and high thermal stability. The formation of TiSi_2 on Si by thin film reaction is often considered for source or drain contacts on Si metal-oxide-semiconductor device structures.^{1–5}

TiSi_2 exhibits two different phases, a stable C54 phase with an orthorhombic face centered structure and a metastable C49 phase with an orthorhombic base centered structure. Previous studies have shown that the Si atoms diffuse into the Ti and react to initially form the C49 TiSi_2 phase. It is established that the metastable C49 TiSi_2 films formed at low temperatures ($<700^\circ\text{C}$) contain substantial faulting and other microstructural defects. After annealing at higher temperatures ($>700^\circ\text{C}$), the TiSi_2 transforms to the stable C54 phase, which has a lower sheet resistivity and a much lower defect density than the C49 phase.^{6–8} Thus, the question arises as to whether the low resistivity is intrinsic to the C54 phase or due to the lower defect density.

Also accompanying the C54 phase transition is the tendency towards island formation.^{2,6,9,10} For films produced with 200 Å of Ti or less, islanding is readily observed at annealing temperatures of $750\text{--}900^\circ\text{C}$.⁹ This effect can significantly degrade the sheet resistivity of the C54 phase of TiSi_2 films less than 400 Å thick.¹¹ While the effect is less significant for films formed with greater than 400 Å of Ti on Si, the need for shallow junctions on the source and drain regions of metal-oxide-semiconductor field-effect transistor devices requires thinner metal layers while not sacrificing the contact or sheet resistivity.^{12,13} For thin TiSi_2 films on Si there is only a narrow temperature range in which to obtain low resistivity while avoiding the formation of islands. Alternatively, a laser processing technique was recently used in TiSi_2 thin film deposition, which does not require the high temperature annealing.¹⁴ The technique demonstrates smooth film surfaces, but the process is not self-aligned, and further high temperature processes may be inevitable during devices fabrication. In order not to be limited by this narrow temperature range for processing, a different approach was tried in this study. If the C49 phase of TiSi_2 films can be stabilized at higher annealing temperatures, a C49 phase with a lower

defect density and therefore a lower sheet resistivity may be obtained.

In previous studies from this laboratory, it has been proposed that the stability of the C49 phase of TiSi_2 is related to its low surface and interface free energies.^{9,10} Since the C54 phase is the stable phase in the binary phase diagram, this phase must exhibit a lower bulk free energy. It has also been reported that reacted films with the C54 phase have much lower strain than films in the C49 phase, and it is possible that the strain may also contribute the stabilization of the C49 phase.¹⁵ Thus, it may be possible to codeposit Ti with a small amount of another metal element to stabilize the C49 phase of the film. The C49 phase formed in this way may be stable to higher annealing temperatures without transforming to the high surface energy C54 phase. In this study, alloying of TiSi_2 with a small amount of Zr was studied to determine if the C49 phase could be stabilized. Since both Ti and Zr are in the group IVb transition metal column, the elements exhibit many chemical similarities, and Zr seems to be the optimal choice to be alloyed with Ti. Films formed from the reaction of Zr and Si to form ZrSi_2 also exhibit a relatively low electrical resistivity ($35\text{--}40\ \mu\Omega\text{ cm}$) and a high thermal stability.¹⁶ More important, ZrSi_2 has only one stable phase, namely the C49 structure.^{16,17}

The experiments described here were carried out in an integrated film growth/characterization system. Three chambers from that system used in this study included the deposition system, a chamber with low-energy electron diffraction (LEED) and Auger electron spectroscopy (AES) capability, and a chamber for Raman spectroscopy. The base pressure of the transfer line of the system is 3×10^{-9} Torr. Before the Ti-Zr deposition, *n*-type Si(111) substrates were cleaned by exposure to UV/ozone irradiation to remove hydrocarbon contamination from the surface, and HF-based spin etch to remove the native oxide, and followed by heat cleaning to 850°C for 10 min in the ultrahigh vacuum (UHV) chamber to desorb hydrogen and other residues.^{18,19} The *in situ* LEED pattern of the cleaned substrates exhibited a 7×7 Si(111) reconstructed structure, and AES showed no detectable carbon or oxygen on the surface prior to the deposition. The base pressure in the UHV chamber was $<5\times 10^{-10}$ Torr. The Ti and Zr alloy films were codeposited

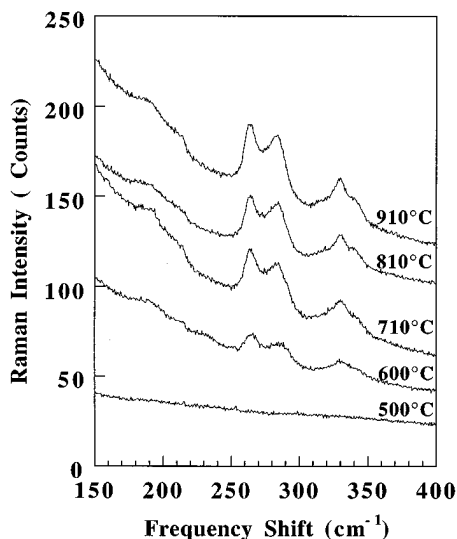


FIG. 1. Raman spectra of 200 Å $\text{Ti}_{0.9}\text{Zr}_{0.1}$ film on Si(111) annealed at temperatures from 500 to 910 °C.

on the atomically cleaned Si(111) substrates by electron beam evaporation with the substrates at room temperature. The total thickness of the alloy metal films was 200 Å. The compositions of the alloy films were selected by controlling the deposition rate of the Ti and Zr sources. The films were then annealed *in situ* at temperatures between 500 and 910 °C.

It has previously been shown that Raman spectroscopy can be used to distinguish between the C49 and C54 phases of TiSi_2 .²⁰ Raman spectra were excited with ~ 200 mW of 514.5 nm Ar ion laser radiation. The laser spot on the samples was $\sim 200 \mu\text{m} \times 2$ mm. The scattered light was first filtered with a subtractive 0.32 m double monochromator and then dispersed with a 0.64 m spectrometer. The light was detected with a LN_2 cooled multichannel charge coupled device detector. Figure 1 shows the *in situ* Raman spectra of a 200 Å $(\text{Ti}_{0.9}\text{Zr}_{0.1})$ alloy film on Si(111) annealed from 500 to 910 °C. The annealing time was 20 min in each case. The features displayed in the range of 250–350 cm^{-1} of the 600–910 °C spectra can all be assigned to the C49 TiSi_2 structure.⁹ The broad features in the range of 180–220 cm^{-1} of the spectra are artifacts of the spectrometer used and have been observed in the spectra of many of the samples analyzed with this spectrometer. No signal was observed at $\sim 240 \text{ cm}^{-1}$ where features associated with the C54 phase are located.^{9,20} From the signal to noise ratio in the data, the volume fraction of any C54 component is estimated to be less than 10%. The Raman results indicate that the transition temperature from the C49 phase to the C54 phase is greater than 910 °C for the 200 Å $(\text{Ti}_{0.9}\text{Zr}_{0.1})$ alloy films on Si(111), which is more than 200 °C higher than the previous observed transition temperature for TiSi_2 films on Si(111) with the same thickness.

The surface roughness and surface morphologies of the samples were studied using atomic force microscopy (AFM). The AFM used for this experiment was a Park Scientific

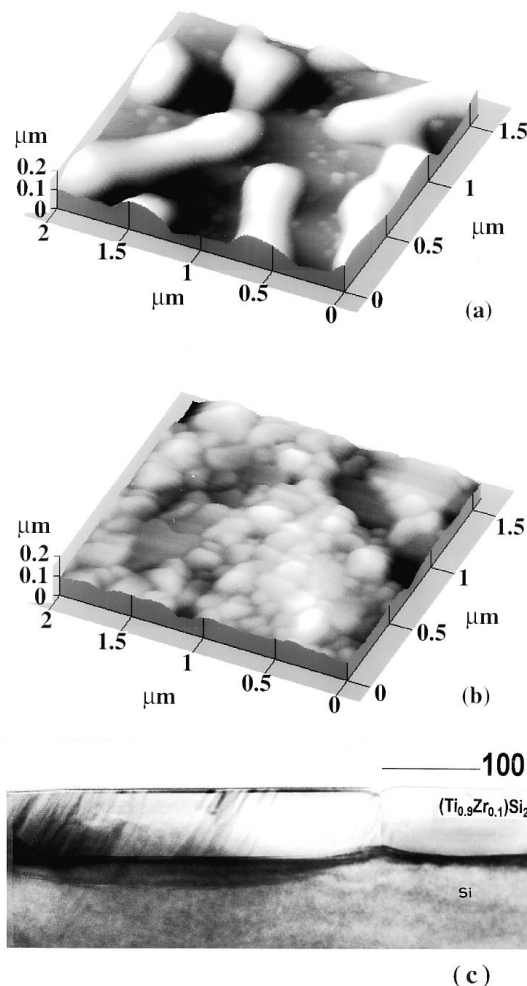


FIG. 2. (a) AFM image of 200 Å Ti/Si film annealed at 900 °C. (b) AFM image of 200 Å $\text{Ti}_{0.9}\text{Zr}_{0.1}$ /Si film annealed at 910 °C. (c) Cross-section TEM micrograph of 200 Å $\text{Ti}_{0.9}\text{Zr}_{0.1}$ /Si film annealed at 910 °C.

SFM-BD2. The piezoscanner used for this experiment had a 10 μm scanning range in both the X and Y directions and a 2.5 μm range in the Z direction. The scan area on the sample surfaces was $\sim 2 \mu\text{m} \times 1.6 \mu\text{m}$. As shown in Fig. 2, in contrast with TiSi_2 thin films, the $(\text{Ti}_{0.9}\text{Zr}_{0.1})\text{Si}_2$ alloy disilicide films with the C49 phase consisted of many small grains. The grains cover the Si substrate uniformly, and transmission electron microscopy results also shown in Fig. 2 indicate a relatively smooth interface with the Si substrate. The sizes of the grains increase as the annealing temperature is increased. The diameters of the grains are $\sim 0.1 \mu\text{m}$ for the film annealed at 600 °C and up to $\sim 0.4 \mu\text{m}$ for the film annealed at 910 °C. No island formation was observed at temperatures less than 910 °C. For each image, the mean surface level (in the Z direction) was calculated and removed from the images before the rms surface roughness was calculated. Shown in Fig. 3 is the temperature dependence of the rms surface roughness for the 200 Å $(\text{Ti}_{0.9}\text{Zr}_{0.1})$ alloy films on Si. The surface roughness results for the TiSi_2 and ZrSi_2 films are also plotted for comparison. We note that the ZrSi_2 results were obtained from a film formed with 100 Å Zr, and we expect that the rms roughness should scale with thickness.

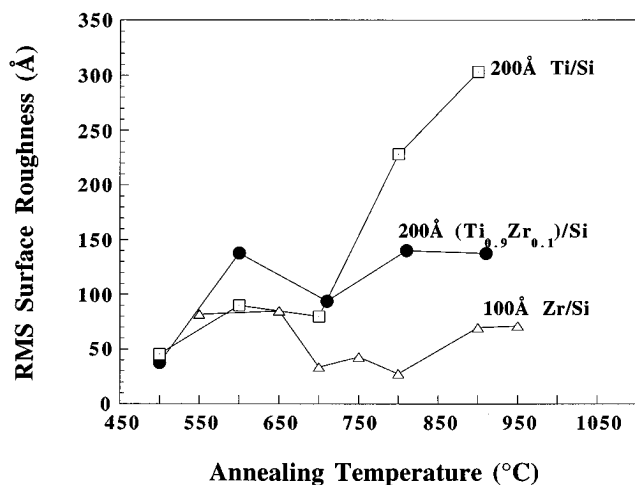


FIG. 3. The rms surface roughness results of the $(\text{Ti}_{0.9}\text{Zr}_{0.1})/\text{Si}$, Ti/Si , and Zr/Si films obtained from the AFM measurements at different annealing temperatures.

The rms roughness of the $(\text{Ti}_{0.9}\text{Zr}_{0.1})\text{Si}_2$ films is significantly less than that of the TiSi_2 films at temperatures above 700 °C.

The sheet resistance of the alloy films were measured using a four-point probe. The results are shown in Fig. 4. The C49 $(\text{Ti}_{0.9}\text{Zr}_{0.1})\text{Si}_2$ alloy films annealed at high temperatures (>600 °C) have a much lower sheet resistance ($\sim 9.9 \Omega/\square$) than the film annealed at 500 °C. The sheet resistance of the C49 phase remains almost unchanged from 600 to 910 °C. Although higher than the resistance of the C54 TiSi_2 films on $\text{Si}(111)$ annealed at 700 °C ($\sim 4.0 \Omega/\square$) and 800 °C ($\sim 7.9 \Omega/\square$), the resistance of the C49 $(\text{Ti}_{0.9}\text{Zr}_{0.1})\text{Si}_2$ alloy films is much lower than the resistance of the TiSi_2 films annealed at 900 °C ($25.3 \Omega/\square$). The sheet resistivity of the C49 $(\text{Ti}_{0.9}\text{Zr}_{0.1})\text{Si}_2$ alloy films is calculated to be $\sim 46 \mu\Omega \text{ cm}$, which is higher than the lowest sheet resistivity of TiSi_2 films

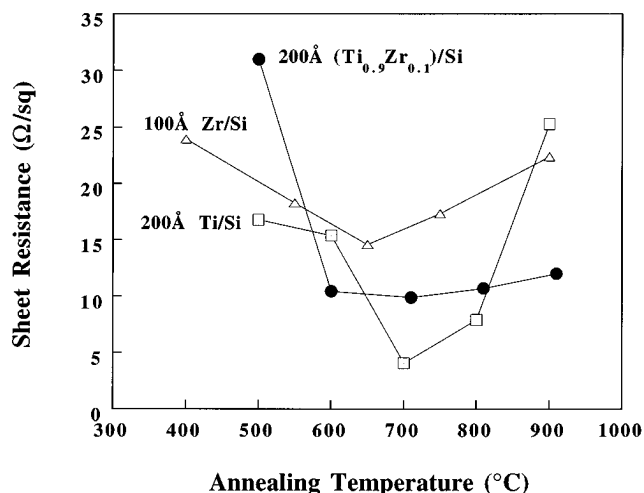


FIG. 4. Sheet resistances results of the $(\text{Ti}_{0.9}\text{Zr}_{0.1})/\text{Si}$, Ti/Si , and Zr/Si films at different annealing temperatures.

($\sim 18 \mu\Omega \text{ cm}$). The sheet resistance of the $(\text{Ti}_{0.9}\text{Zr}_{0.1})\text{Si}_2$ films is also lower than that of the C49 TiSi_2 films annealed at 500 and 600 °C. For comparison, the sheet resistances of $\text{Ti}-\text{Zr}$ alloy films on Si with 20% and 5% Zr were also measured. The $(\text{Ti}_{0.8}\text{Zr}_{0.2})\text{Si}_2$ films have slightly higher ($\sim 30\%$) sheet resistances than those of the $(\text{Ti}_{0.9}\text{Zr}_{0.1})\text{Si}_2$ films over the temperature range studied. The increase of the sheet resistance as the Zr composition is increased may be due to alloy scattering effects. The $(\text{Ti}_{0.95}\text{Zr}_{0.05})\text{Si}_2$ alloy films have the same sheet resistance as the $(\text{Ti}_{0.9}\text{Zr}_{0.1})\text{Si}_2$ alloy films for annealing temperature below 910 °C. At 910 °C, however, the sheet resistance of the $(\text{Ti}_{0.95}\text{Zr}_{0.05})\text{Si}_2$ increases dramatically, and the AFM measurements indicate that islands have formed. The results confirm the original suggestion that the island formation would occur at higher temperature when the Zr alloy composition is increased.

We also note that the sheet resistance of the C49 $(\text{Ti}_{0.9}\text{Zr}_{0.1})\text{Si}_2$ alloy is significantly less than that usually observed for C49 TiSi_2 . This indicates that a large contribution of the increased resistance of the C49 TiSi_2 is likely due to the presence of defects and stacking faults. The higher annealing temperatures used to form the C49 alloy silicides apparently results in a reduced density of defects and stacking faults.

We thank D. B. Aldrich, M. Joo, Z. Wang, and C. A. Sukow for their invaluable help. This work is supported in part by the National Science Foundation through Grant No. DMR 9204285, and the US Department of Energy, Division of Material Science under Contract No. DE-FG05-89ER45384.

- ¹ S. P. Murarka, J. Vac. Sci. Technol. **17**, 775 (1980).
- ² C. Y. Ting, S. S. Iyer, C. M. Osburn, G. L. Hu, and A. M. Schweighart, in *The Use of TiSi_2 in Self-Aligned Silicide Technology*, edited by C. J. Dell'Oca and W. M. Bullis (The Electrochem. Society, Pennington, NJ, 1981), p. 224.
- ³ R. A. Haken, J. Vac. Sci. Technol. B **3**, 1657 (1985).
- ⁴ M. E. Alperin, T. C. Hollaway, R. A. Haken, C. D. Gosmeyer, R. V. Karnaugh, and W. A. Parmantie, IEEE Trans. Electron. Devices **ED-32**, 41 (1985).
- ⁵ K. Maex, Mater. Sci. Eng. **R11**, 53 (1993).
- ⁶ R. Beyers and R. Sinclair, J. Appl. Phys. **57**, 5240 (1985).
- ⁷ T. C. Chou, C. Y. Wong, and K. N. Tu, J. Appl. Phys. **62**, 2275 (1987).
- ⁸ L. F. Mattheiss and J. C. Hensel, Phys. Rev. B **39**, 7754 (1989).
- ⁹ H. Jeon, C. A. Sukow, J. W. Honeycutt, G. A. Rozgonyi, and R. J. Nemanich, J. Appl. Phys. **71**, 4269 (1992).
- ¹⁰ C. A. Sukow and R. J. Nemanich, J. Mater. Res. **9**, 1214 (1994).
- ¹¹ C. Y. Ting, F. M. d'Heurle, S. S. Iyer, and P. M. Fryer, J. Electrochem. Soc. **133**, 2621 (1986).
- ¹² A. H. Perera and J. P. Krusius, Appl. Phys. Lett. **57**, 1410 (1990).
- ¹³ K. Ng and W. T. Lynch, IEEE Trans. Electron. Devices **ED-34**, 503 (1987).
- ¹⁴ P. Tiwari, M. Longo, G. Matera, S. Sharan, P. L. Smith, and J. Narayan, J. Electron. Mater. **20**, 775 (1991).
- ¹⁵ Y. Dao, A. M. Edwards, D. E. Sayers, and R. J. Nemanich, in *Silicides, Germanides and Their Interfaces*, edited by R. W. Fathauer, L. Schowalter, S. Mantl, and K. N. Tu [Mater. Res. Soc. Symp. Proc. (in press)].
- ¹⁶ T. Yamauchi, S. Zaima, K. Mizuno, H. Kitamura, Y. Koide, and Y. Yasuda, J. Appl. Phys. **69**, 7050 (1991).
- ¹⁷ J. Y. Chen and L. J. Chen, J. Appl. Phys. **68**, 4002 (1990).
- ¹⁸ D. B. Fenner, D. K. Biegelsen, and R. D. Bringans, J. Appl. Phys. **66**, 419 (1989).
- ¹⁹ T. Takahagi, I. Nagai, A. Ishitani, H. Kuroda, and Y. Nagasa, J. Appl. Phys. **64**, 3516 (1988).
- ²⁰ R. J. Nemanich, R. T. Fulks, B. L. Stafford, and H. A. Vander Plas, Appl. Phys. Lett. **46**, 670 (1985).